the plant journal

SEB Society for Experimental Biology

The Plant Journal (2011) **65**, 1–14 doi: 10.1111/j.1365-313X.2010.04399.x

CalS7 encodes a callose synthase responsible for callose deposition in the phloem

Bo Xie[1], Xiaomin Wang[1], Maosheng Zhu[1,2], Zhongming Zhang[2] and Zonglie Hong[1,*]

[1]*Department of Microbiology, Molecular Biology and Biochemistry, University of Idaho, Moscow, ID 83844, USA, and*

[2]*State Key Laboratory of Agricultural Microbiology, Huazhong Agricultural University, Wuhan 430070, China*

Received 1 May 2010; revised 13 August 2010; accepted 31 August 2010; published online 9 November 2010.

*For correspondence (fax +1 208 885 6518; e-mail zhong@uidaho.edu).

SUMMARY

It has been known for more than a century that sieve plates in the phloem in plants contain callose, a β-1,3-glucan. However, the genes responsible for callose deposition in this subcellular location have not been identified. In this paper we examine callose deposition patterns in T-DNA insertion mutants (*cs7*) of the *Callose Synthase 7* (*CalS7*) gene. We demonstrated here that the *CalS7* gene is expressed specifically in the phloem of vascular tissues. Callose deposition in the phloem, especially in the sieve elements, was greatly reduced in *cs7* mutants. Ultrastructural analysis of developing sieve elements revealed that callose failed to accumulate in the plasmodesmata of incipient sieve plates at the early perforation stage of phloem development, resulting in the formation of sieve plates with fewer pores. In wild-type Arabidopsis plants, callose is present as a constituent polysaccharide in the phloem of the stem, and its accumulation can also be induced by wounding. Callose accumulation in both conditions was eliminated in mature sieve plates of *cs7* mutants. These results demonstrate that *CalS7* is a phloem-specific callose synthase gene, and is responsible for callose deposition in developing sieve elements during phloem formation and in mature phloem induced by wounding. The mutant plants exhibited moderate reduction in seedling height and produced aberrant pollen grains and short siliques with aborted embryos, suggesting that *CalS7* also plays a role in plant growth and reproduction.

Keywords: ***Arabidopsis thaliana,*** **callose, wound, vascular tissue, sieve plate.**

INTRODUCTION

The vascular system, consisting of xylem and phloem, connects all parts of the plant, from the root system through the stem into leaves and developing seeds. In the stem of Arabidopsis, the xylem and phloem tissues are differentiated from the meristematic procambium cells that form a band sandwiched between the xylem and the phloem. In addition to providing physical support for the plant body, the xylem tissue is responsible for the transport of water and soluble mineral nutrients. The phloem is the 'food and information superhighway' of the plant, responsible for long-distance transport of carbohydrates, amino acids, RNA, proteins, fatty acids, hormones and other signaling molecules (Ruiz-Medrano *et al.*, 2001; van Bel *et al.*, 2002; Ye, 2002). Both xylem and phloem tissues contain various cell types, which can vary depending on growth and developmental stage (Carlsbecker and Helariutta, 2005; Evert, 2006). Recent studies have uncovered genes and pathways involved in the patterning and function of the vascular system (Bonke *et al.*, 2003; Fukuda, 2004; Sieburth and Deyholos, 2006; Dettmer *et al.*, 2009). However, the molecular mechanisms underlying the differentiation and functional regulation of the phloem tissue structures are poorly understood.

In angiosperms, the basic components of the phloem are the sieve elements and parenchyma cells. Other morphologically and physiologically specialized cells such as fibers, sclereids, laticifers and resin ducts can also be present in the phloem. The sieve elements, the primary conducting unit of the phloem, comprise longitudinal sieve tube elements and smaller adjacent companion cells, both of which are derived from the same precursor cells of sieve elements (Evert, 2006). The companion cells contain the nucleus with active cellular activities and play a pivotal role in functional regulation of the enucleate sieve tube elements (Sjölund, 1997; Oparka and Turgeon, 1999). As they mature, the sieve tube elements undergo profound organelle degeneration including the breakdown of the nucleus, vacuoles, rough endoplasmic reticulum (ER) and Golgi, giving rise to an effective path for transport. At maturity, the sieve tube elements retain a plasma membrane and a reduced number

© 2010 The Authors
The Plant Journal © 2010 Blackwell Publishing Ltd

of organelles including ER, plastids and mitochondria. The maturation of sieve tube elements also involves perforation of the cell wall, giving rise to the formation of the sieve plate and sieve areas. The sieve tube elements are linked end-to-end by the sieve plate, a unique specialized porous area of the cell wall. The side wall of sieve tube elements can also develop specialized porous zones, known as sieve areas, which are responsible for lateral transport. Sieve pores of the sieve plate and sieve areas are developed from the plasmodesmata. The process of sieve pore development is poorly understood, and the role of callose in this process is controversial.

Callose is a β-1,3-glucan that can be synthesized and degraded in a timely manner during plant development (Verma and Hong, 2001). It is believed that callose is deposited in the form of platelets around the plasmodesmata of the cell wall between two sieve element cells. This newly deposited callose is used to replace the cellulosic wall material surrounding the plasmodesmata (Evert, 2006). Upon dissolution of the callose and removal of the middle lamella cell wall material, a plate structure with widened pores is developed. According to this model, the amount of deposited callose may govern the final physical size of the sieve pores. Throughout sieve pore development, the ER remains pressed against the plasma membrane near the plasmodesmatal region, but is removed when the pore attains its final size. A drastic amount of callose deposition around the sieve pores can also be rapidly induced by mechanical injury, chemical treatments and physiological stress conditions (Sjölund, 1997; Evert, 2006), which has been used as evidence to argue against a role for callose in sieve pore development. According to this theory, the detected presence of callose around the sieve pores is simply an artifact resulting from the response to sampling injury and chemical fixation. Thus, the molecular mechanism underlying callose biosynthesis and regulation in phloem remains an unanswered question in plant cell biology.

In Arabidopsis, there are 12 *Callose Synthase* genes (*CalS*; EC 2.4.1.34; UDP-glucose:1,3-β-D-glucosyl transferase). Multiple *CalS* genes appear to have evolved in plants to meet the need to produce callose in different tissues and in response to a range of biotic and abiotic stresses (Verma and Hong, 2001; Dong *et al.*, 2008). CalS1 and CalS10 have been shown to be responsible for cell plate formation (Hong *et al.*, 2001a,b; Thiele *et al.*, 2008; Chen *et al.*, 2009; Guseman *et al.*, 2010). CalS5, CalS9, CalS10, CalS11 and CalS12 play unique roles during the process of microsporogenesis and pollination (Dong *et al.*, 2005; Enns *et al.*, 2005; Nishikawa *et al.*, 2005; Töller *et al.*, 2008; Huang *et al.*, 2009; Xie *et al.*, 2010). CalS12 can be induced by pathogen infection and wounding (Jacobs *et al.*, 2003; Nishimura *et al.*, 2003; Dong *et al.*, 2008). The physiological roles of the remaining *CalS* genes in Arabidopsis are still unknown.

The fact that sieve plates are rich in callose has been known for a century (Hartig, 1851; Eschrich, 1956), but the genetic pathway responsible for callose deposition in this location is poorly understood. The callose level in developing vascular tissues is reduced in mutant plants defective in the *ALTERED PHLOEM DEVELOPMENT* (*APL*) gene, which encodes a MYB factor required for phloem differentiation in Arabidopsis (Bonke *et al.*, 2003). Callose of the sieve plates is reduced significantly in the double mutant of the phloem-specific *Sucrose Synthase* (*SuSy*) 5 and 6 (Barratt *et al.*, 2009). Although these studies may have provided new evidence for metabolically influenced regulation of callose synthesis, the genes responsible for phloem-associated callose biosynthesis are still unknown. In this paper we provide genetic and anatomical evidence for a role for CalS7 in callose deposition in the phloem.

RESULTS

Isolation of *CS7* mutants

Four independent mutant lines with T-DNA insertion in the *At1g06490* locus (Figure 1a), SALK_048921 (*cs7-1*), SAIL_114_A01 (*cs7-2*), SAIL_232_C06 (*cs7-3*) and SALK_040051 (*cs7-4*), were obtained from the Arabidopsis Biological Resource Center (ABRC) and grown in greenhouse conditions. Genomic DNA, prepared from individual plants of each line, was used for the identification of homozygous mutant lines by genomic PCR using primers corresponding to the *CalS7* gene and to the T-DNA (Figure 1b and S1a in Supporting Information, Table S1). Homozygous mutant lines were characterized with regards to their growth and reproduction phenotypes, ultrastructures of the phloem and callose deposition. The RT-PCR results showed that the *cs7* mRNA could not be detected in homozygous mutant plants (Figures 1c and S1b), suggesting that they represent knockout mutants at the *CalS7* locus.

Cloning of the *CalS7* cDNA

We cloned the *CalS7* cDNA (GenBank accession number HM049631) by PCR using RNA isolated from the wild-type plants. The full-length coding sequence (CDS) is 5802 bp and may encode a polypeptide of 1933 amino acid residues. Consistent with the other reported CalS peptides, CalS7 contains the highly conserved putative catalytic domain in the C-terminal half of the polypeptide (underline, Figure S2). Its N-terminal 500 amino acids represent a relatively unique domain in the CalS family. Whereas all studied CalS peptides contain 16 predicted transmembrane domains (TMDs), CalS7 may have 18 predicted TMDs (Figures 1d,e and S2). The two unique TMDs are located in the N-terminal 550 amino acid region. Because this protein is likely to be present in the sieve plate of the phloem, these two unique TMDs may play a role in targeting to this unique subcellular location.

© 2010 The Authors

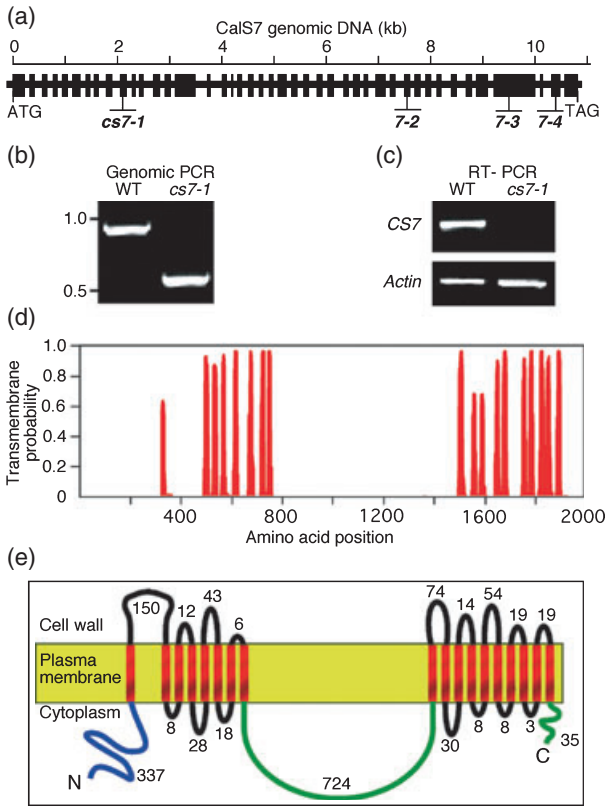

Figure 1. Mutants of *cs7* and predicted topology of the CalS7 protein.
(a) Diagram showing the genomic structure of the *CalS7* gene and the T-DNA insertion sites. Black boxes represent exons and lines represent introns. Exons were determined from comparison of *CalS7* cDNA (GenBank accession number HM049631) and its genomic DNA sequences. Triangles indicate the T-DNA insertion sites.
(b, c) Genomic PCR (b) and RT-PCR (c) of homozygous *cs7-1* lines. *Actin2* PCR product was used as an internal control.
(d, e) Transmembrane helices predicted by the TMHMM program (TMHMM Server at http://www.cbs.dtu.dk/services/TMHMM/) and topology of CalS7 in the membrane. Numbers indicate the amino acid residues of the non-membrane-spanning segments.

Growth and reproduction defects of *cs7* mutants

Under normal greenhouse conditions, plants of the four *cs7* mutant lines exhibited similar growth phenotypes. They were significantly shorter than WT plants (Figure 2a). This growth defect could be observed in 5–8-week-old plants and resulted from a reduction in the length of the stem in *cs7* lines, as no significant difference was detected in the rosette leaf development in the early growth stages. The *cs7* mutant plants produced shorter siliques that contained aborted embryos (Figure 2b). The fertility of *cs7* pollen grains was significantly reduced. This was probably caused by the loss of pollen vitality as evaluated by Alexander stain (arrowheads, Figure 2c). Mature *cs7* pollen grains also tended to clump together in quartets (Figures 2c and S1c). This pollen phenotype may suggest that *CalS7* also plays a role in pollen development. When germinated on an agar plate containing MS medium, *cs7* mutant seedlings developed much shorter roots than wild-type controls (Figures 2d and S3). This seedling growth defect could be partially rescued by supplementation of 1% glucose to the MS medium (Figures 2d and S3). How this partial rescue of growth defect by glucose was brought about remains to be resolved. These observations demonstrate the important roles of the *CalS7* gene in plant development and reproduction.

Phloem-specific expression of *CalS7*

We performed a quick survey of the expression pattern of *CalS7* by RT-PCR, which showed that *CalS7* is expressed widely in all plant organs including the stem, roots, leaves, flowers and siliques (Figure 3a). To further understand the tissue specificity of *CalS7* gene expression, we examined transgenic Arabidopsis plants expressing a β-glucuronidase reporter under the control of the *CalS7* gene promoter, $CalS7_{PRO}$::GUS (Figure 3b). GUS activity was detected specifically in the vascular system of all plant organs examined (Figure 3c–k). Further analysis of the stem and leaf sections revealed that *CalS7* is a phloem-specific gene and is not expressed in the xylem tissue (Figure 3c–f). Strong GUS activity could be detected in both sieve elements and companion cells (Figure 3d). Analysis of *in situ* hybridization using a labeled *CalS7* mRNA probe also confirmed the presence of *CalS7* gene expression in the phloem cells of the vascular tissue (Figure S4b). This tissue specificity of gene expression implicates that *CalS7* may be involved in callose biosynthesis in the phloem.

Lack of callose deposition in the vascular system of *cs7* mutants

In order to test if callose deposition in various plant tissues would be altered in *cs7* mutants, we used aniline blue dye to stain leaves, stem, roots and flowers of 4–5-week-old plants prepared with the routine sampling and fixation method described in Experimental Procedures. We were able to detect callose in the pollen mother cells, microspore tetrads, pollen tubes, root hair tips, megaspores and cell plates of dividing root cells in *cs7* mutants as in the control plants (Figure S5). However, the levels of callose deposition in the vascular system of leaves, roots, stem and flowers were significantly reduced (Figure 4). Callose deposition in the stem and peduncle was mainly detected in the phloem of vascular tissues in wild-type plants, but was absent in *cs7* mutants (Figures 4e,f and S1d). In order to determine if this lack of phloem-callose was unique to *cs7*, we tested for the presence of callose in the phloem tissue of available mutants defective in other *CalS* genes, including homozygous mutants of *cs1*, *cs5*, *cs10* and *cs12*, as well as *heterozygous cs9/+* that produces no homozygous mutant progeny due to the male gametophytic lethality (Xie *et al.*, 2010). We found that callose accumulation in the phloem of leaves and stem

© 2010 The Authors

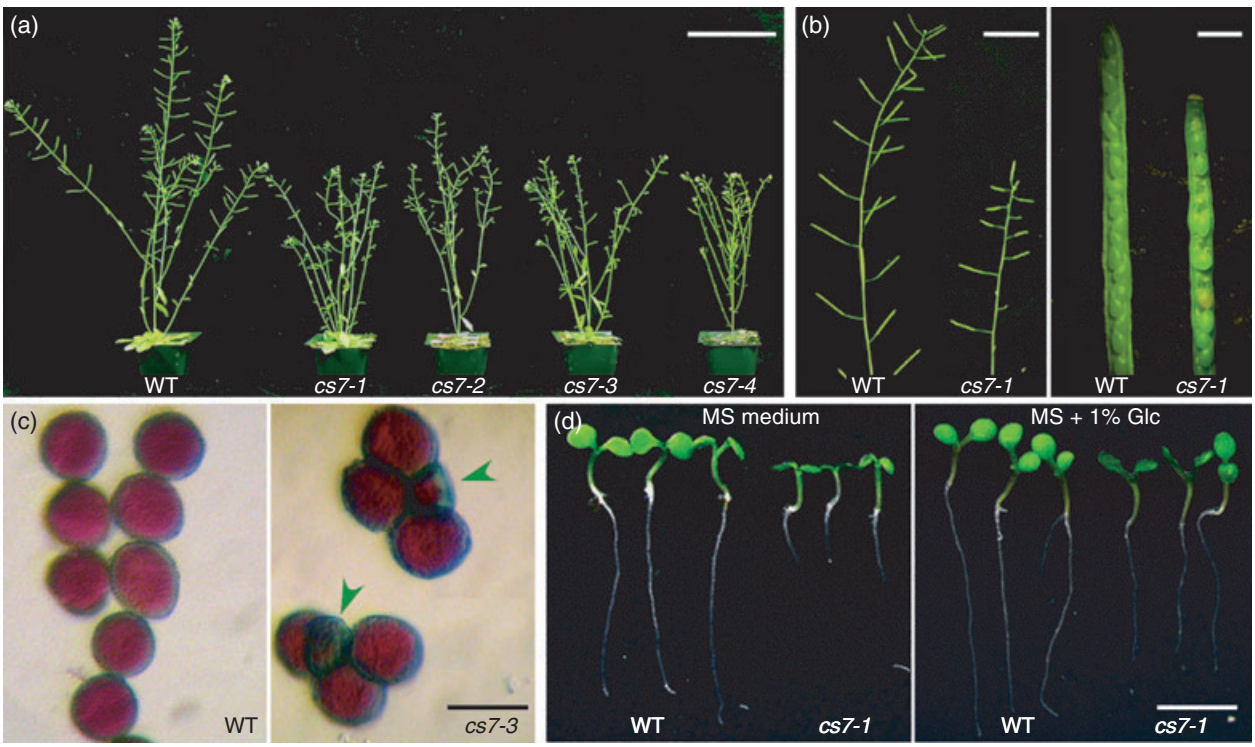

Figure 2. Vegetative growth and reproduction phenotypes of *cs7* mutants.
(a) Six-week-old plants of wild type (WT) and *cs7* mutants.
(b) Siliques of *cs7* mutants were short and contained aborted embryos.
(c) Clumping of mature *cs7* pollen grains as compared with complete separation of individual WT pollen. Arrows indicate non-viable pollen that appeared as deformed and greenish grains stained with Alexander solution.
(d) Retarded growth of 5-day-old *cs7* seedlings germinated on Murashige and Skoog (MS) agar medium (Murashige and Skoog, 1962). This growth defect could be rescued partially by supplementation of the MS agar medium with 1% glucose.
Scale bars: 10 cm (a), 1.5 cm (b, left), 2 mm (b, right), 10 μm (c), 5 mm (d).

was not affected in *cs1*, *cs5*, *cs10*, *cs9/+* and *cs12* (Figure S6). *CalS12* is known to be responsible for callose accumulation in leaf mesophyll cells around the wounding sites generated by mechanical damage and pathogen infection (Jacobs *et al.*, 2003; Nishimura *et al.*, 2003; Dong *et al.*, 2008). Our result shows that while *CalS12* is indeed responsible for wound-induced callose accumulation in the mesophyll cells, it plays no role in wound-induced callose deposition in the phloem (Figure S6a). Thus, *CalS7* is specifically required for callose biosynthesis in the phloem.

We also applied the modified pseudo-Schiff propidium iodide (mPS-PI) staining technique for the visualization of internal tissue structures in Arabidopsis (Truernit *et al.*, 2008), coupled with aniline blue staining, to investigate callose deposition in the sieve elements of phloem under a confocal microscope. In the wild-type plant, callose deposits were found largely associated with the sieve plate (Figure 5a–c). In a longitudinal section of the stem in the control plants, callose is deposited at the sieve plate in a plug-like pattern that covered the tooth-like structure of sieve pores (Figure 5d,e). Callose was also detected in the side cell wall of the sieve elements, possibly at the sites of the sieve areas (Figure 5b,c, arrowheads) and plasmodesmata (Figure 5b,c, punctate light-blue spots), which serve as communication channels between the sieve element and its companion cells. In *cs7* mutants, however, callose was rarely detected in the sieve plate and the side cell wall of the sieve elements (Figure 5f–j). The plug-like pattern of callose was absent from the sieve plate of the mutant plants (Figure 5i,j). Coincidently, the tooth-like structure of sieve pores was also poorly formed (Figure 5i,j), suggesting that the *CalS7* gene is required for the deposition of callose at the sieve pores as well as for the development of the pore structure of sieve elements.

Aberrant pore structures of callose-less sieve plates

In the wild-type plants, sieve plates in a transverse view contained easily recognizable pores at a density of $2.7 \pm 0.5\ \mu m^{-2}$ ($n = 10$), which were covered with plenty of callose deposits (Figure 6a–c, Type I). Callose-positive sieve plates (Figure 6a–c, Types I and II) were rarely detected in *cs7* mutants. Some sieve plates of the *cs7* mutants might develop seemly normal pores, but not as many ($1.6 \pm 0.3\ \mu m^{-2}$, $n = 10$) and with only remnant

© 2010 The Authors

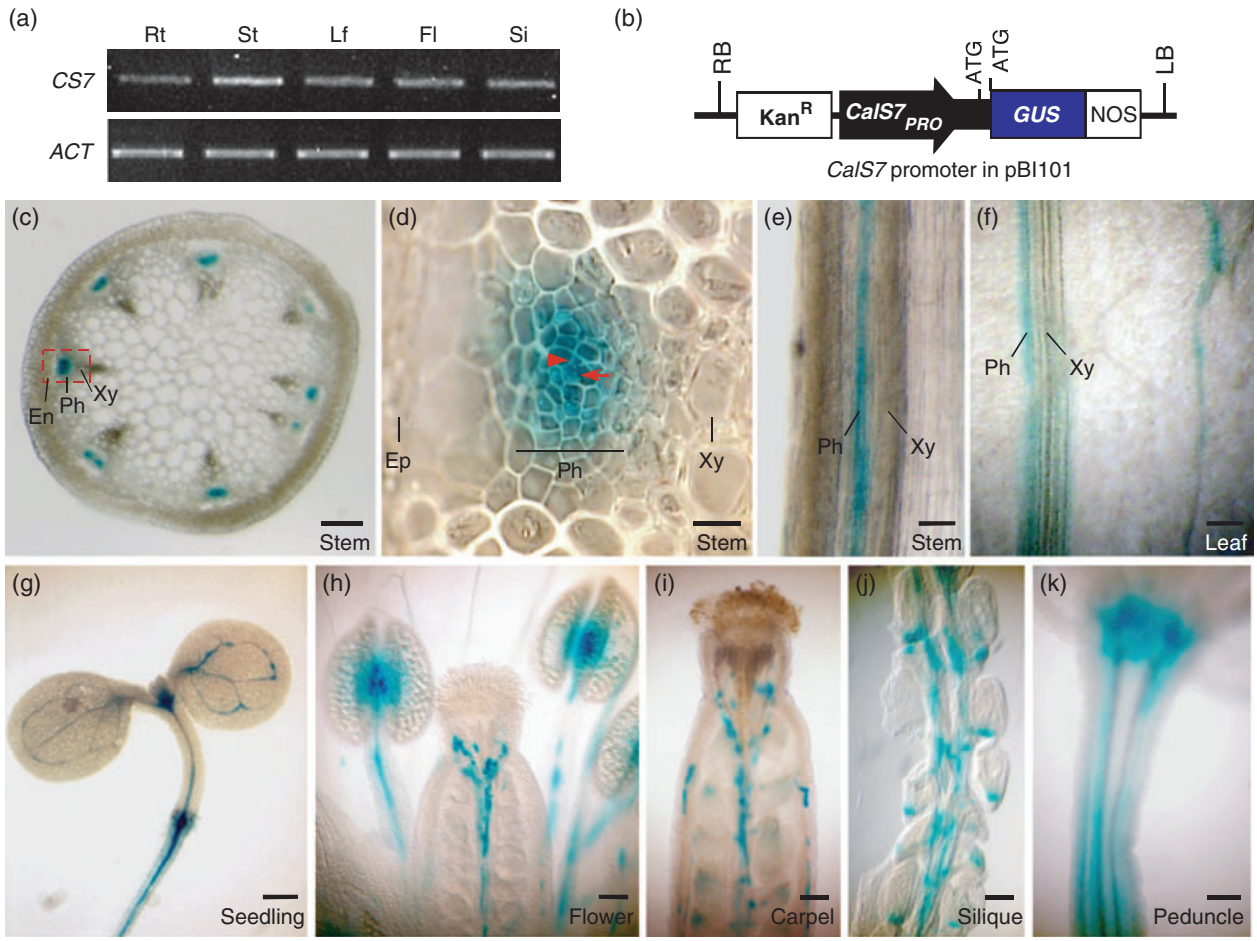

Figure 3. Expression pattern of the *CalS7* gene.
(a) RT-PCR showing the expression levels of the *CalS7* (*CS7*) mRNA in different plant tissues. Rt, root; St, stem; Lf, leaf; Fl, flower; Si, silique. *ACT*, RT-PCR products of *Actin 2* mRNA used as an internal control.
(b) *CalS7*$_{PRO}$::GUS construct. A 2 kb fragment of the *CalS7* gene including the promoter, 5′-untranslated region (UTR) and the first 20 codons was fused in frame with the *uid* (GUS) coding region.
(c–k) Expression analysis of *CalS7*$_{PRO}$::GUS in different plant tissues. GUS activity was detected in the vascular system of the stem (c–e), leaf (f), root and seedling (g), flower (h), silique (i), seed (j) and peduncle (k). GUS activity was specifically detected in the phloem of stem cross-sections (c, d), and stem and leaf longitudinal sections (e, f). High GUS activity was detected in the sieve elements (arrow) and companion cells (arrowhead) as shown in (d).
En, endodermis; Ph, phloem; Xy, xylem. Scale bars: 300 μm (c, g), 40 μm (d, h–k), 100 μm (e, f).

callose deposits (Type II). Most sieve plates of the *cs7* mutants were callose-less, and had either only a few tiny pore-like structures (Type III), or a strong reaction with PI dye but no recognizable pores at all (Type IV). In wild-type plants, Type IV structures accounted for approximately 10% of the sieve plates, while no Types II and III were detected (Figure 6a,c). In contrast, no Type I sieve plates could be found in *cs7* mutants, suggesting that mutations at the *CalS7* gene not only affected callose deposition to the sieve plates but also disturbed the formation of the sieve pores.

Aberrant sieve plate structure in the *cs7* mutant

Callose is believed to play a role in the differentiation of sieve pores from plasmodesmata during the development of sieve elements (Esau and Thorsch, 1985). We examined the ultrastructure of sieve plates at different developmental stages by transmission electron microscopy (TEM). In the shoot apical region immediately below the apical meristem, where sieve elements were still in their early development stages, the plasmodesmata of the incipient sieve plates at the perforation stage were surrounded with thick layers of callose in the control plants (Figure 7a). In *cs7* mutants, however, the plasmodesmata of perforating sieve plates (Figure 7b) or of the newly developed sieve plates (Figure 7c) contained no callose. Without callose present, the differentiation of the plasmodesmata to sieve pores appeared to be hampered in *cs7* mutants, resulting in the formation of sieve plates with fewer, abnormally developed pores (see below).

In mature sieve plates in the control plants, the cell wall consisted of three distinct layers distinguishable on the

© 2010 The Authors

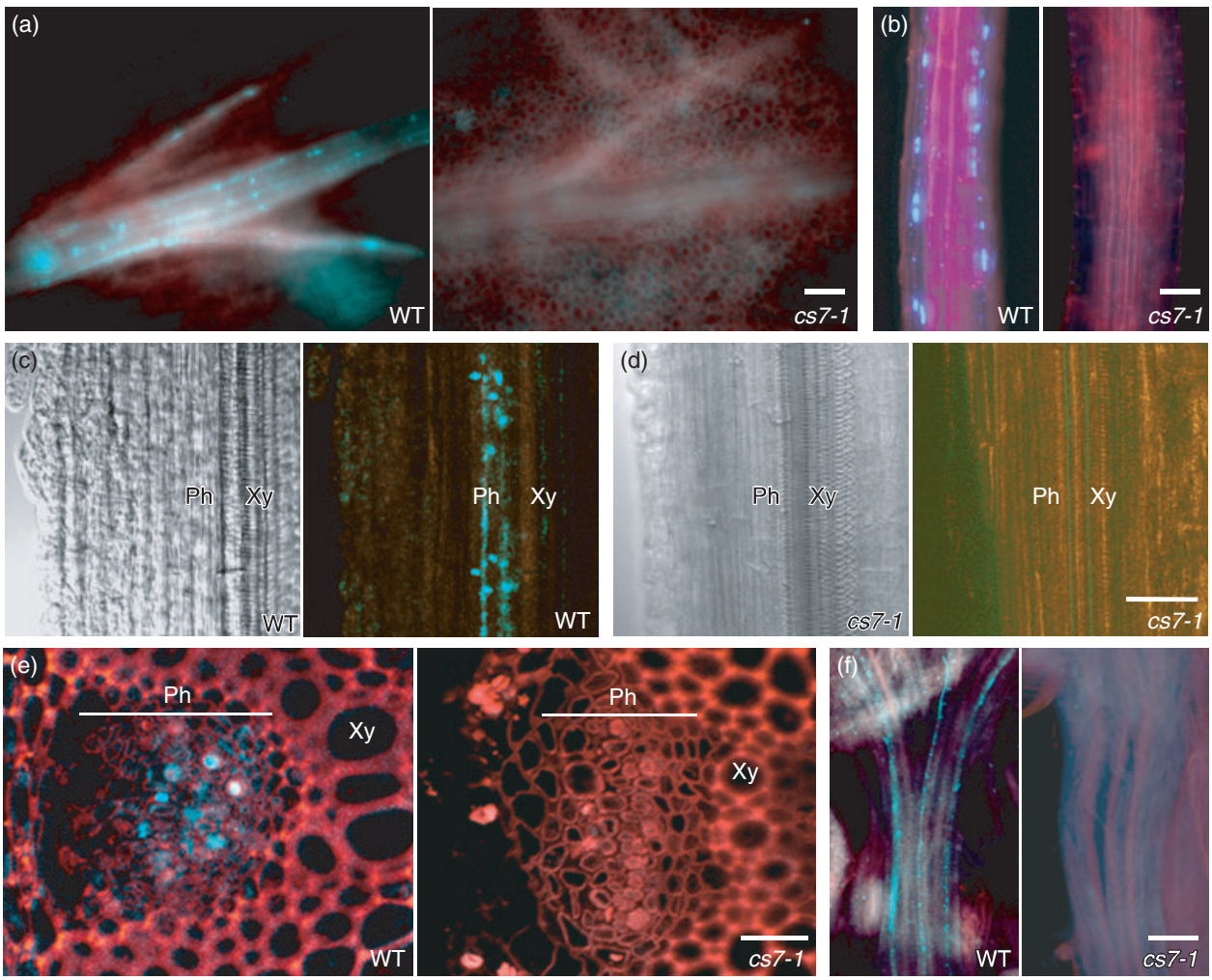

Figure 4. Lack of callose deposition in the vascular tissues of *cs7* mutants.
Tissues of the leaf (a), root (b), stem (c–e) and peduncle (f) were fixed and stained with aniline blue (a–d, f) or aniline blue and propidium iodide (PI) (e). Fluorescence images (a, b, c right, d right, f) were generated by superimposing fluorescence images of callose (light blue) using a UV filter and autofluorescence background (red) taken using a TRITC filter. The characteristic spiral thickenings of the tracheids on the bright-field images of the stem (c, d left) serve as indicators of the xylem. Confocal images of stem cross-sections (e) were generated by merging the images for callose (light blue) with a filter set of 405 nm excitation and 480–520 nm emission, and the images for PI staining (red) taken using 515 nm excitation and 560–660 nm emission.
Ph, phloem; Xy, xylem. Scale bars: 40 μm (a, e), 30 μm (b), 100 μm (c, d), 80 μm (f).

basis of electron density of the cell wall material. In the middle of the sieve plate cell wall lies the electron-dense middle lamella (Ml), a pectin-rich layer cementing the two adjacent sieve elements. Primary cell walls (Pw), the thick electron-light layers comprising primarily cellulose and hemicelluloses, are deposited on each side of the middle lamella. Callose forms a distinctive electron-rare layer (Ca) that surrounds the islands of the sieve plate cell wall. In the control plants, sieve plates contained well-developed sieve pores (diameter 380 ± 47 nm, $n = 12$), which were surrounded by the electron-sucking P-protein (Pp) (Figure 7d,g). By contrast, the cell wall of mature sieve plates in *cs7* did not have the callose layer and had thin primary cell walls (Figure 7e,f,h). Most of the sieve pores of *cs7* mutants were incompletely open (Figure 7e,h) or were very narrow in diameter (Figure 7f,i; diameter 190 ± 32 nm, $n = 12$). In addition, we found that many of the sieve pores in *cs7* were fully occluded with P-protein-like structure aggregates (Figure 7c,i). The elevated level of P-protein-like structure aggregates in *cs7* mutants might compensate for the function of the lost callose deposition in plugging the sieve pores. In the *cs7-2* line, which was a slightly weaker allele and occasionally produced plants with slightly weaker phenotypes, some of the sieve plates were found to contain a residual layer of callose (Figure 7i). Although this residual callose deposition failed to cover the whole sieve plate, it was sufficient to support the development of thicker layers of the primary cell wall (Figure 7i). These data clearly show

© 2010 The Authors

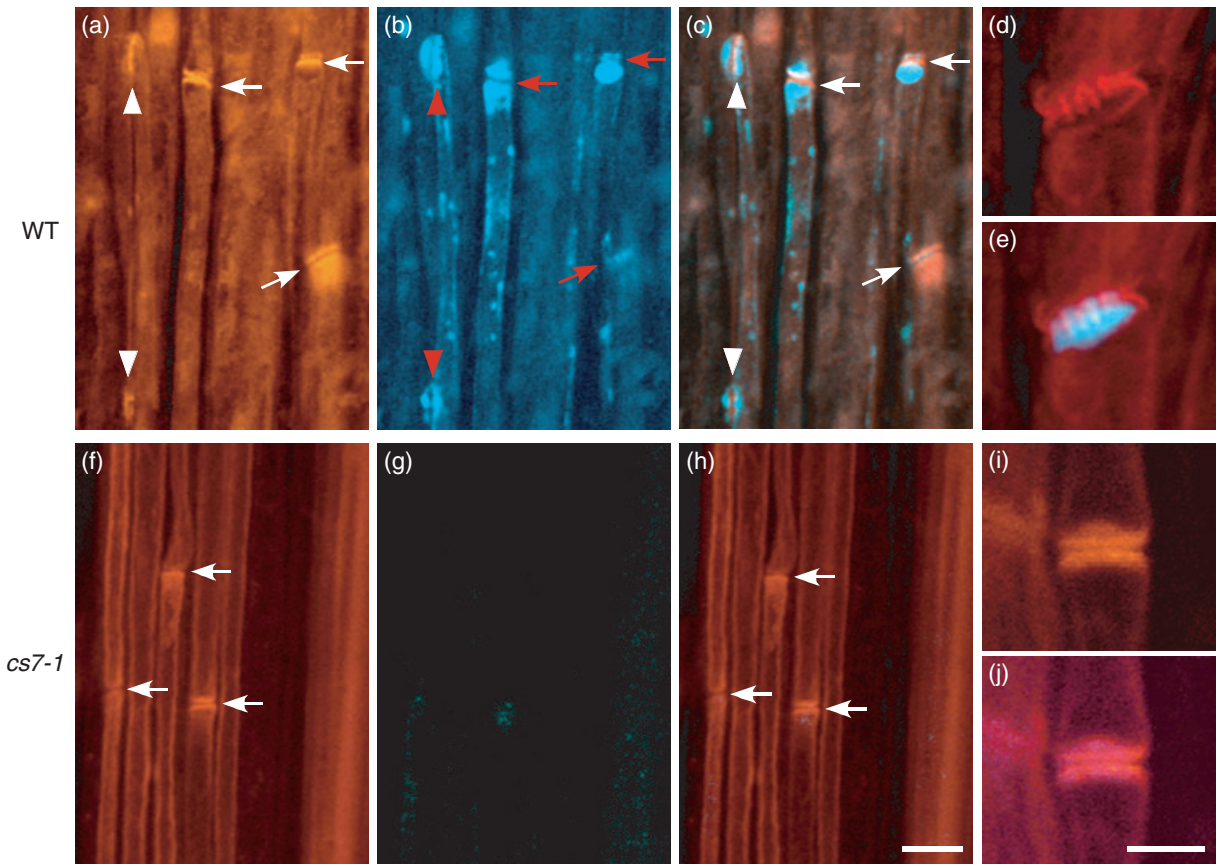

Figure 5. Lack of callose deposition in the sieve plate.
Stem tissues were fixed, cleaned and stained with aniline blue and propidium iodide (PI). Confocal images were taken using 405 nm excitation and 480–520 nm emission to detect callose (light blue), and 515 nm excitation and 560–660 nm emission to detect the PI signal (red).
(a, f) The PI-stained cell wall structures of the sieve elements of a wild-type plant (a) and *cs7* (f) plant.
(b, g) Images of callose deposition in the same views as in (a) and (f).
(c, h) Overlaid images of (a) and (b), and (f) and (g).
(d, i) Enlarged images of the PI-stained sieve plates of a wild-type plant (d) or *cs7* plant (i).
(e, j) Overlaid images of the sieve plates in (d) and (j) with callose deposition. Arrows indicate the positions of the sieve plates. Arrowheads point to the positions of vertical sieve areas.
Scale bars: 10 μm (a–c, f–h), 5 μm (d, e, i, j).

that *CalS7* is required for the deposition of the callose layer of the sieve plate cell wall and for the development of sieve pores.

Lack of wound-induced callose in the phloem in *cs7*

It has long been known that injury and treatment with chemicals can induce callose deposition in plant tissues (Stone and Clarke, 1992; Verma and Hong, 2001). Sampling and chemical fixation might inevitably induce callose deposition in the phloem (Davis and Evert, 1970; Eschrich, 1975). In order to examine the potential role of *CalS7* in wound-induced callose deposition in phloem, we prepared samples that were subjected to different wounding conditions. To reduce the time of exposure to wounding, we immersed the whole intact Arabidopsis plants directly in the fixation solution, or froze the stem samples in liquid nitrogen immediately after excision. To enhance wounding stress, we incubated excised stem samples (0.5 cm) in water-saturated papers for 1–10 min before chemical fixation.

As shown in Figure 8, in the control plants, callose deposition in the vascular tissues, most of which was in the sieve plate, was greatly increased by wounding treatments (Figure 8a). The number of callose-positive sieve plates, as indicated by the fluorescent dots in the low-magnification images (Figure 8), increased from 50–70 mm^{-1} of longitudinal phloem in the control samples (liquid N_2 or intact plant fixation) to 120–150 in the wound-treated samples (1–10 min incubation). The induction of callose deposition in the phloem was a rapid process, because even 1 min of incubation of the excised stems was sufficient to significantly induce callose deposition in the sieve plates in the control plants, which was consistent with a recent report (Mullendore *et al.*, 2010). In *cs7* mutants, however, no significant callose deposition could be detected

© 2010 The Authors

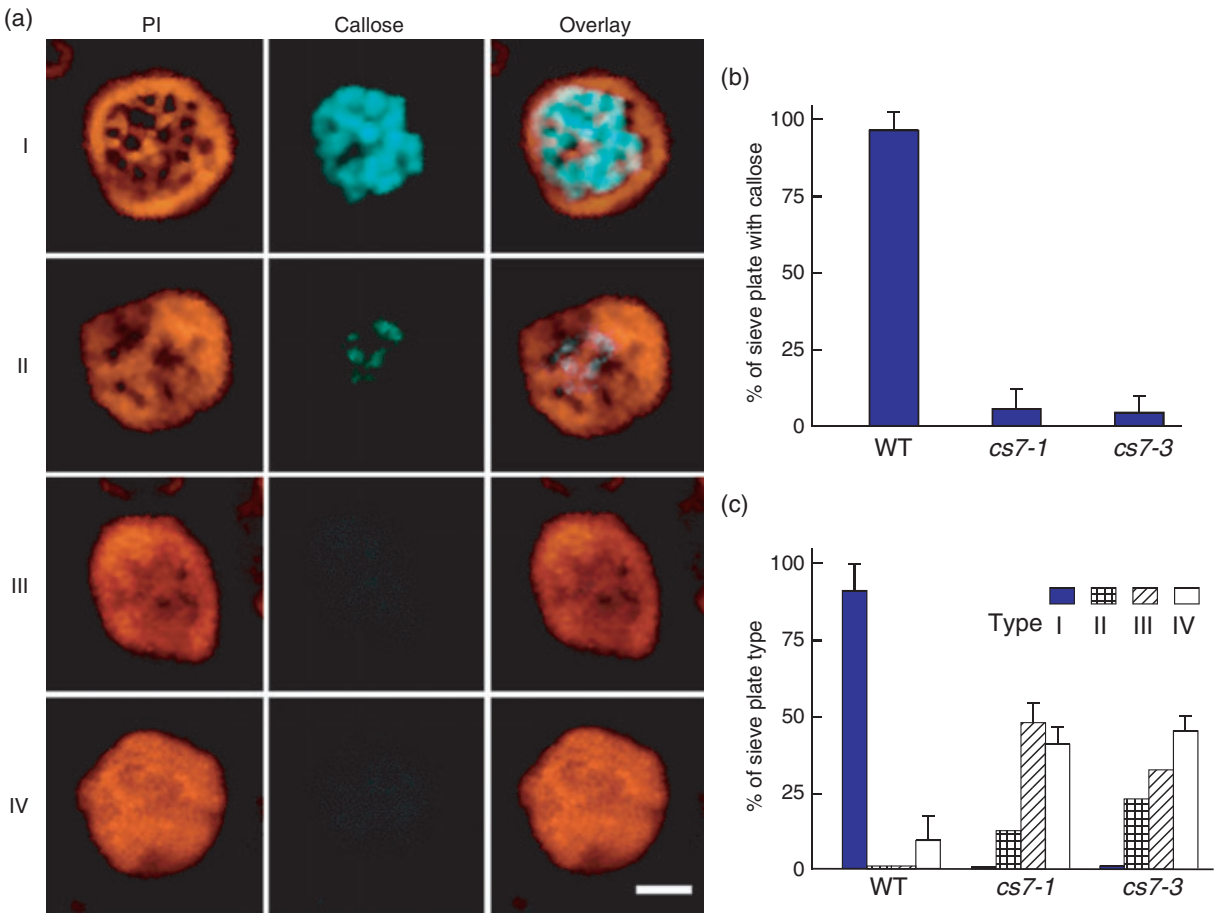

Figure 6. Types of sieve plates and callose deposition.
(a) Confocal images of the sieve plates stained with aniline blue (light blue) and propidium iodide (PI) (red). Type I: normal sieve plates with well-distributed sieve pores and accumulated callose deposits. Type II: sieve plates with a reduced number of pores and remnant callose deposits. Type III: sieve plates with a few pore-like structures and no detectable callose. Type IV: sieve plates with enhanced PI staining, no visible pores and no callose. Scale bar: 2 μm.
(b, c) Percentages of sieve plate showing detectable callose deposition (b) and percentages of different sieve plate types (c) in wild type and *cs7* plants.

in the phloem either under the control conditions or after wound treatment, indicating that *CalS7* is required for the wound-induced callose deposition in the phloem.

We further tested whether the wound-induced callose deposition in the phloem was accompanied by an elevated level of *CalS7* gene transcription. We examined the expression level of the GUS reporter under the control of the *CalS7* gene promoter. Transgenic plants harboring the $CalS7_{PRO}$::GUS construct were subjected to different wound treatments. No significant differences in GUS reporter activity between wound treatments were detected (Figure 8b), suggesting that the transcription of the *CalS7* gene was not induced by wounding. We also verified this result by RT-PCR analysis. No difference in expression level of the *CalS7* mRNA between wounding treatments could be detected. Taken together, these data suggest that the rapid response of callose deposition in the sieve plate under wounding conditions is not due to transcriptional activation of the *CalS7* gene. It remains to be tested if this rapid callose response is a result of activation at the protein/enzyme level.

We also tested whether *CalS7* is required for wound-induced callose deposition in other plant tissues. We stained wound-treated leaves with aniline blue and could detect as much callose deposition around the wounding site in *cs7* mutants as in the wild-type control (Figure S5o,p), suggesting that *CalS7* is not responsible for the wound-induced callose response in leaf epidermal cells. Previously, *CalS12* has been shown to be required for the callose response to mechanical wounding and to pathogen infection (Jacobs *et al.*, 2003; Nishimura *et al.*, 2003; Dong *et al.*, 2008). We therefore wounded *cs12* mutant plants and examined the resulting callose production. We confirmed that leaf epidermal cells of *cs12* mutant plants failed to accumulate callose around the wounding site. However, callose deposition in the sieve plate was not affected by the *cs12* mutation (Figure S6). Thus, we conclude that *CalS7* is responsible for wound-induced callose deposition in the

© 2010 The Authors

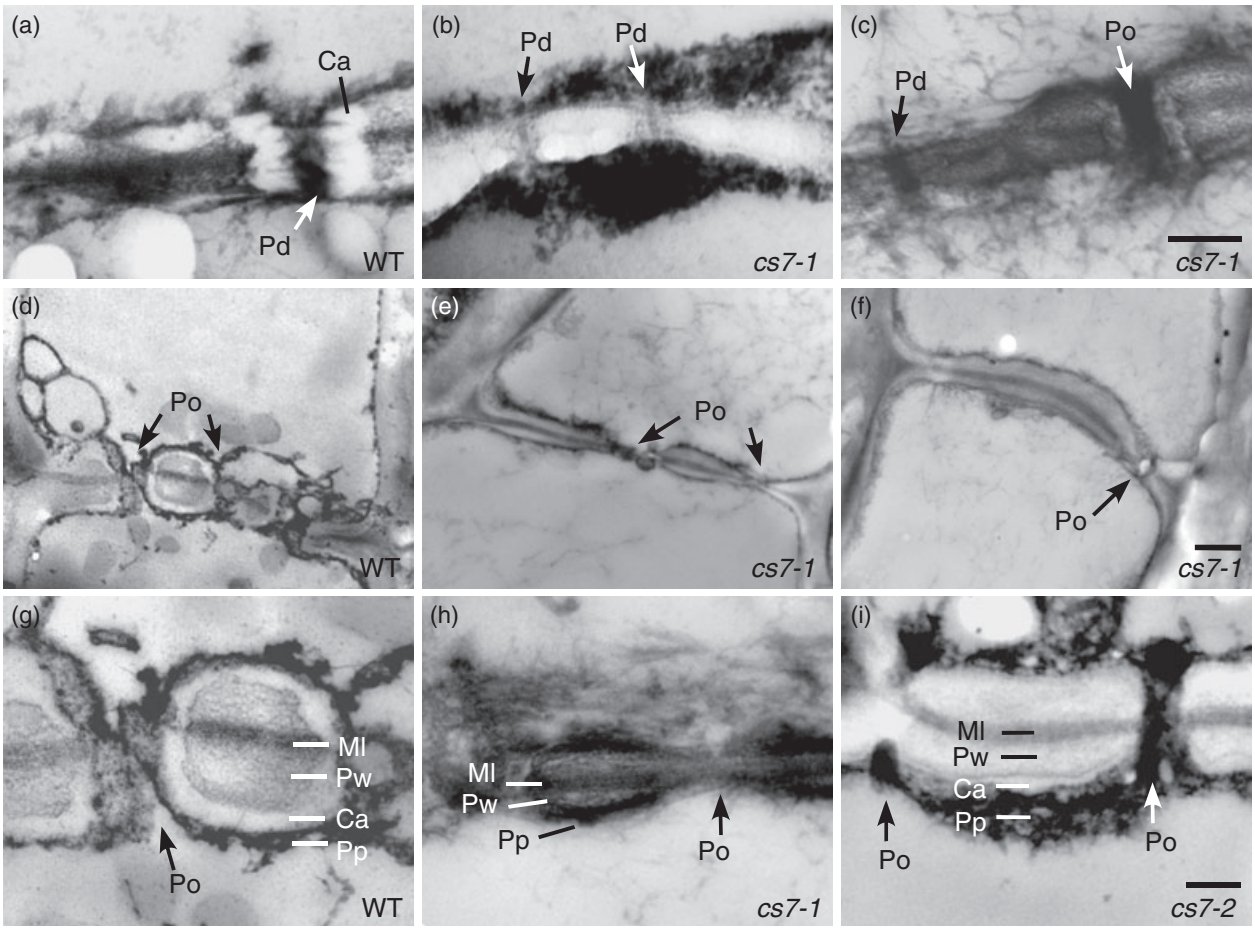

Figure 7. Ultrastructure of sieve plates in *cs7* mutants.
(a, b) Developing sieve plates of a wild-type plant (a) or *cs7* mutant (b) at the perforation stage.
(c) A developing sieve plate of a *cs7* plant with a perforating plasmodesmata canal (Pd) and a newly formed pore (Po).
(d–i) Mature sieve plates of a wild-type plant (d, g) and *cs7* mutant plant (e, f, h, i). Ca, Callose; Ml, middle lamella; Pp, P-protein-like structure; Pw, primary wall.
Scale bars: 250 nm (a–c, g–i), 500 nm (d–f).

phloem, whereas *CalS12* is involved in the callose response in leaf epidermal cells treated with physical wounds or pathogens. These results clearly demonstrate that members of the *CalS* family have unique biological functions and are regulated in a tissue-specific manner as well as in response to various environmental cues.

DISCUSSION

Callose can be easily detected in plant tissues with an epifluorescence microscope, thanks to its characteristic reaction with the fluorescent dye aniline blue. Its presence in the vascular tissues of the stem was observed more than a century ago (Hartig, 1851; Eschrich, 1956; Stone and Clarke, 1992). Wound-induced callose deposition in the phloem has also been examined extensively (Evert and Derr, 1964; Eschrich, 1975). Callose plays a pivotal role in sieve plate development, and in controlling the phloem transport in response to wounding and other endogenous and exogenous signals. In this study we characterized four homozygous T-DNA insertion mutant lines of *cs7*. The *cs7* mRNA could not be detected in the mutant plants (Figures 1c and S1b), suggesting that the T-DNA insertions may have resulted in the formation of unstable or size-altered *cs7* mRNA. We examined the growth and reproduction phenotypes of *cs7* mutant plants and observed changes in callose deposition in association with the *cs7* mutation. Our genetic and cell biology evidence clearly demonstrates that CalS7 is a phloem-specific CalS isoform and is responsible for callose biosynthesis in the sieve elements during phloem development and for the induced callose accumulation in response to wounding signals in the mature vascular tissues of the stem. These data shed new light on the function of a callose synthase gene in phloem development and provide a new molecular tool and target for future studies of stem development and transport in the vascular tissues.

© 2010 The Authors

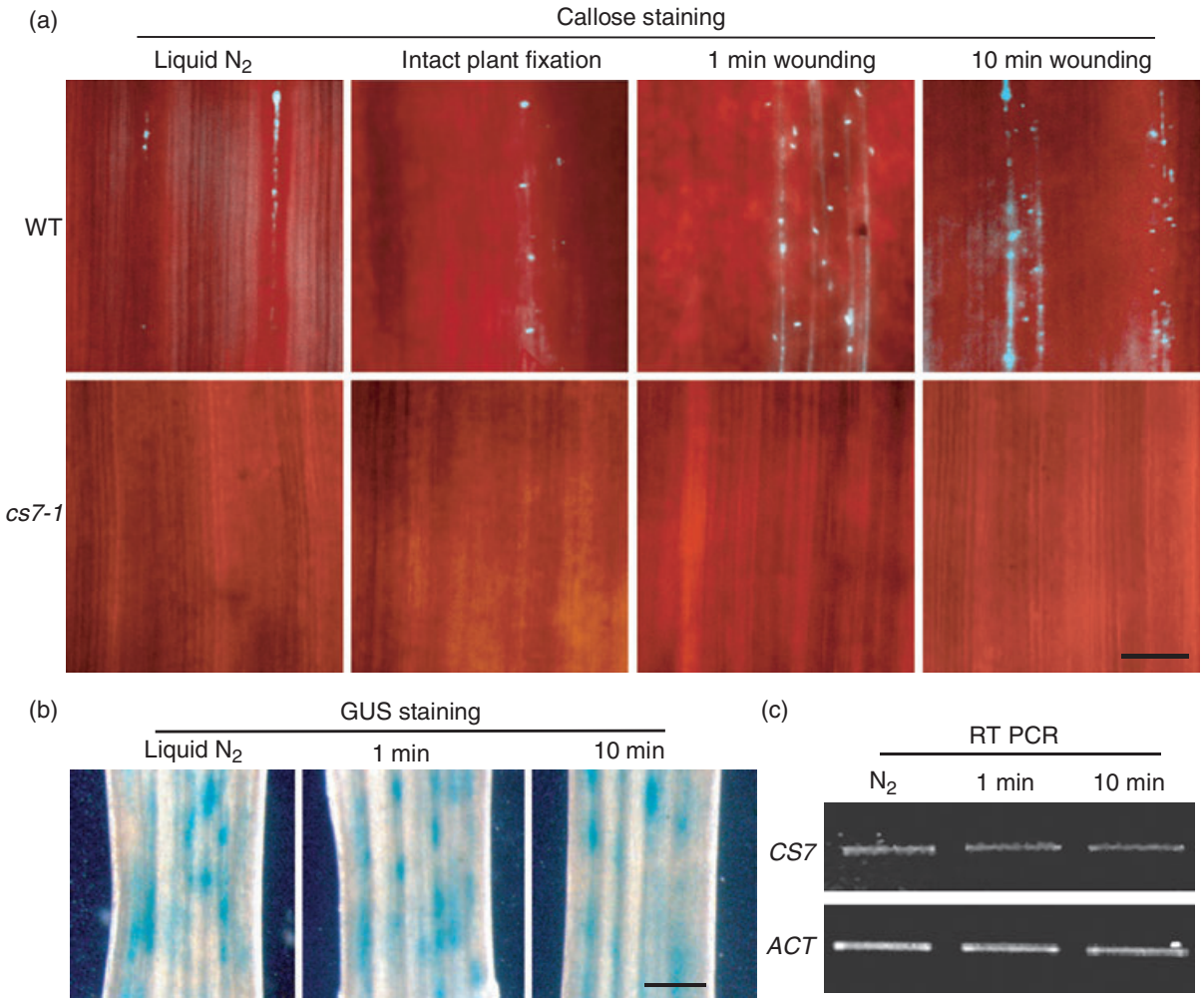

Figure 8. Wound-induced callose deposition in vascular tissues of the stem.
(a) Callose deposition in the vascular tissue induced by wound treatments. The control samples were prepared by freezing with liquid N_2 immediately after stem excision (N_2) or by fixing intact plants directly in fixation buffer (intact plant fixation). For wound treatments, excised fragments (0.5 cm) of the stem were placed on water-saturated paper for 1 min and 10 min. The frozen specimens were then kept in the ECA fixation buffer and stained with aniline blue. Overlaid fluorescence images were generated by merging the images of callose staining (light blue) with autofluorescence background (red). Scale bars: 50 μm.
(b) Expression levels of the GUS reporter in the stem of transgenic plants harboring *CalS7*$_{PRO}$:GUS treated with wounding. Scale bar: 400 μm.
(c) A RT-PCR analysis of the expression levels of the *CalS7* mRNA in the stem samples treated with different wound conditions.

A family of highly tissue specific *CalS* genes

Arabidopsis contains 12 *CalS* genes that were named on the basis of their sequence similarity with CalS1, the first CalS identified in plants (Hong *et al.*, 2001a). Multiple *CalS* genes appear to have evolved in plants to meet the need for callose synthesis in different tissues and in response to a range of biotic or abiotic stresses (Verma and Hong, 2001). Previous studies performed by our group and other laboratories have suggested that CalS1 is responsible for the synthesis of the nascent callose present at the cell plate during cytokinesis (Hong *et al.*, 2001a,b). CalS5 is highly expressed during microsporogenesis, microgametogenesis and pollination, and is responsible for the biosynthesis of the callose wall, pollen tube wall and callose plugs of growing pollen tubes (Dong *et al.*, 2005, 2008; Nishikawa *et al.*, 2005; Xie *et al.*, 2010). CalS9 and CalS10 are highly expressed during pollen formation, but are not responsible for callose wall biosynthesis. CalS9 is required for both symmetric and asymmetric mitosis during male gamete development (Töller *et al.*, 2008; Xie *et al.*, 2010). CalS10 is required for the asymmetric mitosis during microgametogenesis in the another (Thiele *et al.*, 2008; Töller *et al.*, 2008) and during stomatal formation in leaves (Chen *et al.*, 2009; Guseman *et al.*, 2010). The callose wall formed during microsporogenesis can be differentiated into the peripheral wall that surrounds the four microspores in a tetrad and the interstitial callose wall that separates the four microspores. Interestingly, the peripheral

© 2010 The Authors

callose wall is synthesized by CalS5 (Dong *et al.*, 2005, 2008; Nishikawa *et al.*, 2005; Xie *et al.*, 2010), while the biosynthesis of the interstitial wall is dependent on a joint function of CalS11 and CalS12 (Enns *et al.*, 2005). In this study, we demonstrate that *CalS7* is expressed specifically in the phloem of various plant tissues (Figure 3). Loss of the *CalS7* gene resulted in the failure of callose deposition in the sieve elements. The fact that pollen grains of *cs7* mutants clamped together in a tetrad-like manner (Figures 2d and S2c) suggests that *CalS7* might also have a minor role in the formation of the callose wall during pollen formation or the release of microspores from tetrads. This function of *CalS7* is beyond the scope of this work and remains to be exploited in more detail in future work. We also examined callose deposition patterns in the mutant plants of *CalS1*, *CalS5*, *CalS9*, *CalS10* and *CalS12*, and detected no significant alteration in phloem-associated callose deposition (Figure S6). Taken together, these data suggest that *CalS7* is the key isoform of the callose synthases responsible for callose biosynthesis in the phloem.

A role for callose in sieve plate development

During phloem development, the incipient sieve plate is penetrated by densely distributed plasmodesmata. A membranous cylinder, known as the plasmotubule, runs within the plasmodesmal pore and is linked to the cisternae of the ER on both sides of the wall. A thick layer of callose is deposited beneath the plasma membrane around each plasmodesma on both sides of the sieve plate wall. The paired callose deposits, or callose platelets, form a collar that encloses the plasmodesma. The presence of the callose platelets precludes further deposition of cellulose near the plasmadesma. As nuclear degeneration takes place in sieve elements, the cell wall surrounding the plasmadesma begins to be hydrolyzed, resulting in the formation of sieve pores. This perforation process starts with the degradation of the middle lamella followed by the simultaneous removal of the cellulosic primary cell wall and the callose platelets (Deshpande, 1975; Esau and Thorsch, 1985). At the completion of perforation, residual callose remains in the sieve pore area (Ehlers *et al.*, 2000). The ER cisternae may transverse the desmotubule of a single plasmadesma, or remain closely associated with the callose platelets throughout pore development. After the perforation is complete, the ER disappears from the pore areas. It has been proposed that callose may not play a role in the perforation of sieve plates. This view was supported by two lines of evidence obtained from observations of sieve plates in the roots of common duckweed (*Lemna minor*) and sieve areas of gymnosperms. No callose was detected during pore development in these sieve organs (Walsh and Melaragno, 1976). The fact that callose could be induced by wounding during specimen preparation (see below) also complicates the debate on the role of callose. In this study, we took advantage of the *cs7* mutants that could not produce callose during the perforation of sieve plates (Figure 7a–c). Sieve plates formed in *cs7* mutants contained a significantly reduced number of pores per plate (Figure 6) and pore-like structures that did not penetrate through the sieve plates (Figure 7). These lines of genetic and cytological evidence argue strongly for an important role for callose in sieve pore formation.

Wound-induced callose deposition

Mature sieve elements are very responsive to a variety of stimulus cues. Such rapid responses are needed for proper control of mass flow through the phloem, for preventing leakage of the precious translocates and for defense against pathogen infections (Evert, 1982; Verma and Hong, 2001). While the presence of callose in the sieve pores of undisturbed plants remains a topic of debate, wounding, sampling cuts and fixative chemicals such as glutaraldehyde and Ca^{2+} ions can certainly cause significant deposition of callose in mature sieve elements (Hughes and Gunning, 1980; Evert, 1982; Radford *et al.*, 1998; Mullendore *et al.*, 2010). In this study, our data clearly show that callose deposition was eradicated in the phloem of the stem in *cs7* mutants, both before and after wounding treatments (Figures 4–6 and 8). Thus, *CalS7* should be responsible for callose biosynthesis in both developing and mature sieve elements, as well as in mature phloem in response to wound treatments. Wound-induced callose deposition is known to occur within a very short time period (Mullendore *et al.*, 2010). However, how the sieve elements achieve this rapid response in callose accumulation, either at the transcriptional level of *CalS7* expression or by post-translational activation of CalS7 enzyme, remains to be studied in future.

In response to injury, the phloem-specific P-proteins also form filamentous aggregates that rapidly occlude the sieve pores (Ehlers *et al.*, 2000). So long as plants are uninjured, P-proteins are present parietally along the longitudinal walls of sieve elements or in the lumen of sieve elements (Evert *et al.*, 1973; Kollmann, 1980; Evert, 1982; Cronshaw and Sabnis, 1990). However, in injured plants, these proteins become dispersed irregular clots and are concentrated to the sieve pores. The stacked ER cisternae, constituent organelles closely associated with the P-proteins and the callose deposits in mature sieve elements, become detached in injured sieve elements (Schultz, 1992). One of the proposed roles of this ER response could be the release of Ca^{2+} ions (Arsanto, 1986; Sjolund, 1990), which stimulate conformational changes of P-proteins and enhance callose synthase activity (Arsanto, 1986; Verma and Hong, 2001). Our data showed that the P-protein-like structure aggregates were still present in *cs7* mutant (Figure 7). This aggregation appeared to be elevated in some sieve pores of *cs7* mutant (Figure 7), presumably to compensate for the loss of the sieve plate callose.

© 2010 The Authors

Callose biosynthesis in sieve elements

Recent biochemical data (Li *et al.*, 1999; Brownfield *et al.*, 2007) and genetic evidence (Dong *et al.*, 2005; Enns *et al.*, 2005; Nishikawa *et al.*, 2005; Töller *et al.*, 2008; Huang *et al.*, 2009; Guseman *et al.*, 2010) have clearly demonstrated that *CalS* genes encode enzymes that catalyze callose biosynthesis in plants. The CalS proteins containing multiple transmembrane domains are targeted to specific subcellular locations, where their enzyme activities are regulated via interactions with various regulatory proteins and ions (Ca^{2+}) and in response to different developmental and environment signals. We have previously proposed a model of callose biosynthesis at the cell plate (Verma and Hong, 2001), in which phragmoplastin, UDP-glucose transferase (UGT1) and SuSy are proposed to be associated with the cell plate-specific CalS1, (Hong *et al.*, 2001a,b). For callose biosynthesis at the sieve elements, CalS7 is not likely to function alone, but may form a complex with other protein components, such as APL and SuSy5/6, which appear to be involved in callose biosynthesis in phloem (Bonke *et al.*, 2003; Barratt *et al.*, 2009). Additionally, where CalS7 protein is synthesized, how CalS7 is targeted to the sieve plate and how the enzyme activity is regulated by the wound signal, remain to be examined in future work.

A possible role for CalS7 in the development of non-vascular tissues

Previous studies have shown that the loss of certain callose synthases may result in the formation of multiple defects in plant development and in response to environmental signals. In the *cs12* mutant plants, the resistance to pathogen infection is surprisingly enhanced in a salicylic acid-dependent manner (Nishimura *et al.*, 2003). In the *cs9*/+ heterozygous mutants, pollen cell division and pollen germination are altered (Töller *et al.*, 2008; Huang *et al.*, 2009; Xie *et al.*, 2010). CalS10 is found to play multiple roles in pollen development and in stomatal formation (Chen *et al.*, 2009; Guseman *et al.*, 2010). Our observations on *cs7* show that in addition to the lack of phloem callose, other growth and reproduction phenotypes are also associated with the *cs7* mutation, suggesting that CalS7 also plays important roles in plant growth and development. Because the phloem is the main channel for the long-distance transportation of organic nutrients and signal molecules (Ruiz-Medrano *et al.*, 2001; van Bel *et al.*, 2002; Ye, 2002), the loss of callose in sieve elements and the aberrant sieve plate structure observed in *cs7* plants may directly affect transportation in the phloem, which may subsequently cause collateral damage to plant tissue development. How transportation though the phloem is altered in *cs7* remains an interesting topic for future investigations.

Taken together, this study has clearly identified CalS7 as the key CalS enzyme responsible for callose biosynthesis in the phloem, and has provided a very important molecular tool and target for future research in the field of phloem cell development, stress response and vascular transport.

EXPERIMENTAL PROCEDURES

Plant materials

Arabidopsis thaliana ecotype Columbia seeds were germinated on the surface of vermiculite in small pots. Seedlings were transplanted to Metro-Mix 360 (Hummert, http://www.hummert.com/) 14 days post-germination and grown at 21–23°C in a greenhouse.

Genomic DNA extraction and genotyping

Genomic DNA was extracted from the leaves and inflorescence using the cetyl trimethyl ammonium bromide (CTAB) method (Allen *et al.*, 2006). Genotyping of plants was performed by PCR using *CalS7* gene-specific primers and the T-DNA left-border primers (Table S1).

RNA extraction and RT-PCR

Total RNA was extracted using TRIzol reagent (Invitrogen, http://www.invitrogen.com/) and reverse-transcribed into cDNA using the SuperScript First-Strand Synthesis System (Invitrogen). Expression levels of the *CalS7* mRNA and the control *Actin2* were assessed by PCR using the primers shown in Table S1. For PCR amplification, the reaction mix was pre-heated at 94°C for 2 min, followed by 20 cycles of amplification at 94°C, 40 sec, 58°C, 30 sec, and 72°C, 30 sec.

GUS staining

Plant tissues were incubated with GUS staining solution (50 mM sodium phosphate buffer, pH 7.2, 0.05% Triton X-100, 2 mM potassium ferrocyanide, 2 mM potassium ferricyanide, 2 mM 5-bromo-4-chloro-3-indolyl-D-glucuronic acid (Sigma, http://www.sigmaaldrich.com/). Samples were incubated at 37°C for defined times and then cleaned with 70% ethanol.

In situ RNA hybridization

A cDNA fragment of 232 bp corresponding to the mRNA sequence flanking the first ATG of *CalS7* was used to prepare RNA probes labeled with digoxigenin as described elsewhere (Goodrich *et al.*, 1997). The *CalS7* cDNA fragment was amplified by PCR using primers CS75UTR-98F and CS7133R (see Table S1) and cloned into pCRII (Invitrogen). The plasmid was linearized with *Apa*I and transcribed with SP6 RNA polymerase (Roche, http://www.roche.com/) to produce antisense RNA probe. For the preparation of negative control with the *CalS7* sense RNA probe, the plasmid was linearized with *Bam*H1 and transcribed with T7 RNA polymerase (Roche).

Sample preparation and wounding treatments

Plant samples were fixed in ECA fixation buffer (60% ethanol, 30% chloroform, 10% acetic acid), MA buffer (50% methanol, 10% acetic acid) or TEM fixation buffer (2% paraformaldehyde, 2% glutaraldehyde in 50 mM PIPES buffer, pH 7.0). For routine preparations of plant specimens, fresh plant stems were excised in 0.5-cm fragments and immersed in the fixation buffer, which lasted <40 sec from cutting to chemical fixation. For the preparations of the less wounded samples, fresh plant stems were directly frozen in liquid N_2 and excised in 0.5-cm fragments in liquid N_2. The fragments were fixed in the fixation buffer pre-cooled at −20°C. For the preparation of uncut plants, whole seedlings were fixed directly in the fixation buffer for 24 h. The middle fragments of the stem were then excised

© 2010 The Authors

for further analysis. For the preparation of wound-treated samples, excised stems in 0.5-cm fragments were placed on water-saturated paper for 1 min or 10 min, and frozen in liquid N_2 to stop the wound treatment.

Callose staining

For the routine detection of callose in plant tissues, samples were fixed in ECA solution (60% ethanol, 30% chloroform, 10% acetic acid) for at least 2 h, and treated with 2 N NaOH for 5–10 min. After washing with 0.1 M K_2HPO_4, pH 8.5, the specimens were incubated with 0.05% aniline blue (Sigma). For confocal detection of callose deposition, plant samples were fixed in MA solution (50% methanol, 10% acetic acid), and treated with hot ethanol and periodic acid. After staining with PI as described elsewhere (Truernit *et al.*, 2008), the specimens were cleaned with a chloral hydrate solution (4 g chloral hydrate, 1 ml glycerol, 2 ml water) and then stained with 0.05% aniline blue for 10 min.

Microscopy

For epifluorescence microscopy, a UV filter was used to detect the presence of aniline blue-stained callose (blue-yellow fluorescence). Autofluorescence of the sample background (red fluorescence) was imaged with a TRITC filter. Superimposed images of the blue and red fluorescence were created using PHOTOSHOP software (Adobe, http://www.adobe.com).

For confocal microscopy of callose detection, we used an Olympus laser scanning microscope FV1000 (Leeds, http://www.leedsmicro.com) with an excitation filter of 405 nm and emission filter of 485–515 nm. The cell boundary stained with PI was imaged using a set of filters with excitation at 514 nm and emission at 560–660 nm (red fluorescence).

For transmission electron microscopy (TEM), samples were fixed in 2% paraformaldehyde, 2% glutaraldehyde in 50 mM PIPES buffer, pH 7.0, and embedded by infiltration with LR-white resin/ethanol (1 day in 1:3, 1:1 and 3:1, respectively). The specimens were cut into 70-nm ultrathin sections on a Reichert-Jung ultramicrotome (http://www.reichertms.com/). Following uranyl acetate and lead citrate staining, the sections were observed using a Jeol 1200 EX transmission electron microscope (http://www.jeol.com/).

ACKNOWLEDGEMENT

We thank Dr A. Caplan for critical comments on the manuscript, Ms Shizhen Gu for technical assistance and the Franceschi Microscopy and Imaging Center, Washington State University for assistance in transmission electron microscopy. We also thank the ABRC (Ohio State University) for seeds of Arabidopsis T-DNA insertional lines. This work was supported by National Science Foundation grants (MCB-0548525 and IOB-0543923) to ZH, and an National Natural Science Foundation of China grant (NSFC-30870186) to ZZ. MZ was supported by fellowship from the China Scholarship Council (CSC).

SUPPORTING INFORMATION

Additional Supporting Information may be found in the online version of this article:

Figure S1. Consistent phenotypes exhibited in *cs7* alleles.
Figure S2. The *CalS7* gene and its deduced peptide.
Figure S3. Growth and reproduction defects in *cs7* alleles.
Figure S4. *In situ* hybridization of *CalS7* gene expression.
Figure S5. Normal callose deposition in non-vascular tissues of *cs7* mutant plants.
Figure S6. Callose deposition in the phloem of other *cs* mutants.
Table S1. Primers used in this study.

Please note: As a service to our authors and readers, this journal provides supporting information supplied by the authors. Such materials are peer-reviewed and may be re-organized for online delivery, but are not copy-edited or typeset. Technical support issues arising from supporting information (other than missing files) should be addressed to the authors.

REFERENCES

Allen, G.C., Flores-Vergara, M.A., Krasynanski, S., Kumar, S. and Thompson, W.F. (2006) A modified protocol for rapid DNA isolation from plant tissues using cetyltrimethylammonium bromide. *Nat. Protoc.* **1**, 2320–2325.

Arsanto, J.P. (1986) Ca^{2+}-binding sites and phosphatase activities in sieve element reticulum and P-protein of chick-pea phloem: a cytochemical and X-ray microanalysis survey. *Protoplasma*, **132**, 160–171.

Barratt, D.H.P., Derbyshire, P., Findlay, K., Pike, M., Wellner, N., Lunn, J., Feil, R., Simpson, C., Maule, A.J. and Smith, A.M. (2009) Normal growth of *Arabidopsis* requires cytosolic invertase but not sucrose synthase. *Proc. Natl Acad. Sci. USA*, **106**, 13124–13129.

van Bel, A.J.E., Ehlers, K. and Knoblauch, M. (2002) Sieve elements caught in the act. *Trends. Plant Sci.* **7**, 126–132.

Bonke, M., Thitamadee, S., Mahonen, A.P., Hauser, M.T. and Helariutta, Y. (2003) APL regulates vascular tissue identity in *Arabidopsis*. *Nature*, **426**, 181–186.

Brownfield, L., Ford, K., Doblin, M.S., Newbigin, E., Read, S. and Bacic, A. (2007) Proteomic and biochemical evidence links the callose synthase in *Nicotiana alata* pollen tubes to the product of the *NaGSL1* gene. *Plant J.* **52**, 147–156.

Carlsbecker, A. and Helariutta, Y. (2005) Phloem and xylem specification: pieces of the puzzle emerge. *Curr. Opin. Plant Biol.* **8**, 512–517.

Chen, X.Y., Liu, L., Lee, E., Han, X., Rim, Y., Chu, H., Kim, S.W., Sack, F. and Kim, J.Y. (2009) The Arabidopsis callose synthase gene *GSL8* is required for cytokinesis and cell patterning. *Plant Physiol.* **150**, 105–113.

Cronshaw, J. and Sabnis, D.D. (1990) Phloem proteins. In *Sieve Elements: Comparative Structures, Induction and Development* (Behnke, H.D. and Sjolund, R.D., eds). Berlin Heidelberg New York Tokyo: Springer, pp. 257–283.

Davis, J.D. and Evert, R.F. (1970) Seasonal cycle of phloem development in woody vines. *Bot. Gaz.* **131**, 128–138.

Deshpande, B.P. (1975) Differentiation of the sieve plate of *Cucurbita*: a further review. *Ann. Bot.* **39**, 1015–1022.

Dettmer, J., Elo, A. and Helariutta, Y. (2009) Hormone interactions during vascular development. *Plant Mol. Biol.* **69**, 347–360.

Dong, X., Hong, Z., Sivaramakrishnan, M., Mahfouz, M. and Verma, D.P.S. (2005) Callose synthase (CalS5) is required for exine formation during microgametogenesis and for pollen viability in *Arabidopsis*. *Plant J.* **42**, 315–328.

Dong, X., Hong, Z., Chatterjee, J., Kim, S. and Verma, D.P. (2008) Expression of callose synthase genes and its connection with *Npr1* signaling pathway during pathogen infection. *Planta*, **229**, 87–98.

Ehlers, K., Knoblauch, M. and Van Bel, A.J.E. (2000) Ultrastructural features of well-preserved and injured sieve elements: minute clamps keep the phloem transport conduits free for mass flow. *Protoplasma*, **214**, 80–92.

Enns, L.C., Kanaoka, M.M., Torii, K.U., Comai, L., Okada, K. and Cleland, R.E. (2005) Two callose synthases, GSL1 and GSL5, play an essential and redundant role in plant and pollen development and in fertility. *Plant Mol. Biol.* **58**, 333–349.

Esau, K. and Thorsch, J. (1985) Sieve plate pores and plasmodesmata, the communication channels of the symplast: ultrastructural aspects and developmental relations. *Am. J. Bot.* **72**, 1641–1653.

Eschrich, W. (1956) Kallose. *Protoplasma*, **47**, 487–530.

Eschrich, W. (1975) Sealing systems in phloem. In *Encyclopedia of Plant Physiology, Vol. I. Transport in plants. I. Phloem Transport* (M. H. Zimmerman and J. A. Milburn, eds). Berlin: Springer-Verlag, pp. 39–56.

Evert, R.F. (1982) Sieve-tube structure in relation to function. *Bioscience*, **32**, 789–795.

Evert, R.F. (2006) *Esau's Plant Anatomy: Meristems, Cells, and Tissues of the Plant Body: Their Structure, Function, and Development*, 3rd edn. New Jersey: Wiley, pp. 357–405.

Evert, R.F. and Derr, W.F. (1964) Callose substance in sieve elements. *Am. J. Bot.* **51**, 552–559.

© 2010 The Authors

Evert, R.F., Eschrich, W. and Eichhorn, S.E. (1973) P-protein distribution in mature sieve elements of *Cucurbita maxima*. *Planta*, **109**, 193–210.

Fukuda, H. (2004) Signals that control plant vascular cell differentiation. *Nat. Rev. Mol. Cell Biol.* **5**, 379–391.

Goodrich, J., Puangsomlee, P., Martin, M., Long, D., Meyerowitz, E.M. and Coupland, G. (1997) A Polycomb-group gene regulates homeotic gene expression in *Arabidopsis*. *Nature*, **386**, 44–51.

Guseman, J.M., Lee, J.S., Bogenschutz, N.L., Peterson, K.M., Virata, R.E., Xie, B., Kanaoka, M.M., Hong, Z. and Torii, K.U. (2010) Deregulation of cell-to-cell connectivity and stomatal patterning by loss-of-function mutation in Arabidopsis CHORUS (GLUCAN SYNTHASE-LIK 8). *Development*, **137**, 1731–1741.

Hartig, G.L. (1851) *Lehrbuch fur Forster (Neunte Auflage)*. Stuttgart and Tubingen: J.O. Gotta'scher Verlag.'

Hong, Z., Delauney, A.J. and Verma, D.P.S. (2001a) A cell-plate specific callose synthase and its interaction with phragmoplastin. *Plant Cell*, **13**, 755–768.

Hong, Z., Zhang, Z., Olson, J.M. and Verma, D.P.S. (2001b) A novel UDP-glucose transferase is part of the callose synthase complex and interacts with phragmoplastin at the forming cell plate. *Plant Cell*, **13**, 769–779.

Huang, L., Chen, X.Y., Rim, Y., Han, X., Cho, W.Y., Kim, S.W. and Kim, J.Y. (2009) *Arabidopsis* Glucan Synthase-Like 10 functions in male gametogenesis, *J. Plant Physiol.* **166**, 344–352.

Hughes, J.E. and Gunning, B.E.S. (1980) Glutaraldehyde-induced deposition of callose. *Can. J. Bot.* **58**, 250–257.

Jacobs, A.K., Lipka, V., Burton, R.A., Panstruga, R., Strizhov, N., Schulze-Lefert, P. and Fincher, G.B.J. (2003) An *Arabidopsis* callose synthase, *GSL5,* is required for wound and papillary callose formation. *Plant Cell*, **15**, 2503–2513.

Kollmann, R. (1980) Fine structural and biochemical characterization of phloem proteins. *Can. J. Bot.* **58**, 802–806.

Li, H., Bacic, A. and Read, S.M. (1999) Role of a callose synthase zymogen in regulating wall deposition in pollen tubes of *Nicotiana alata*. *Planta*, **208**, 528–538.

Mullendore, D.L., Windt, C.W., Van As, H. and Knoblauch, M. (2010) Sieve tube geometry in relation to phloem flow. *Plant Cell*, **22**, 579–593.

Murashige, T. and Skoog, F. (1962) A revised medium for rapid growth and bioassays with tobacco tissue cultures. *Physiol. Plant*, **15**, 473–497.

Nishikawa, S., Zinkl, G.M., Swanson, R.J., Maruyama, D. and Preuss, D. (2005) Callose (beta-1,3 glucan) is essential for *Arabidopsis* pollen wall patterning, but not tube growth. *BMC Plant Biol.* **5**, 22.

Nishimura, M.T., Stein, M., Hou, B.H., Vogel, J.P., Edwards, H. and Somerville, S.C. (2003) Loss of a callose synthase results in salicylic acid-dependent disease resistance. *Science*, **301**, 969–972.

Oparka, K.J. and Turgeon, R. (1999) Sieve elements and companion cells – traffic control centers of the phloem. *Plant Cell*, **11**, 739–750.

Radford, J.E., Vesk, M. and Overall, R.L. (1998) Callose deposition at plasmodesmata. *Protoplasma*, **201**, 30–37.

Ruiz-Medrano, R., Xoconostle-Cazares, B. and Lucas, W.J. (2001) The phloem as a conduit for inter-organ communication. *Curr. Opin. Plant Biol.* **4**, 202–209.

Schulz, A. (1992) Living sieve cells of conifers as visualized by confocal, laser-scanning fluorescence microscopy. *Protoplasma*, **166**, 153–164.

Sieburth, L.E. and Deyholos, M.K. (2006) Vascular development: the long and winding road. *Curr. Opin. Plant Biol.* **9**, 48–54.

Sjolund, R.D. (1990) Calcium and phloem sieve element membranes. *Curr. Top. Plant Biochem. Physiol*, **9**, 101–118.

Sjölund, R.D. (1997) The phloem sieve element: a river runs through it. *Plant Cell*, **9**, 1137–1146.

Stone, B.A. and Clarke, A.E. (1992) Chemistry and physiology of higher plant 1, 3-β-glucans (callose). In *Chemistry and Biology of (1, 3)-β-Glucans* (Stone, B.A. and Clarke, A.E., eds). Melbourne: La Trobe University Press, Bundoora, Australia, pp. 365–429.

Thiele, K., Wanner, G., Kindzierski, V., Jürgens, G., Mayer, U., Pachl, F. and Assaad, F.F. (2008) The timely deposition of callose is essential for cytokinesis in *Arabidopsis*. *Plant J.* **58**, 13–26.

Töller, A., Brownfield, L., Neu, C., Twell, D. and Schulze-Lefert, P. (2008) Dual function of *Arabidopsis glucan synthase-like* genes *GSL8* and *GSL10* in male gametophyte development and plant growth. *Plant J.* **54**, 911–923.

Truernit, E., Bauby, H., Dubreucq, B., Grandjean, O., Runions, J., Barthélémy, J. and Palauqui, J.C. (2008) High-resolution whole-mount imaging of three-dimensional tissue organization and gene expression enables the study of Phloem development and structure in *Arabidopsis*. *Plant Cell*, **20**, 1494–1503.

Verma, D.P.S. and Hong, Z. (2001) Plant callose synthase complexes. *Plant Mol. Biol.* **47**, 693–701.

Walsh, M.A. and Melaragno, J.E. (1976) Ultralstructural features of developing sieve elements in *Lemna minor* L. – Sieve plate and lateral sieve areas. *Am. J. Bot.* **63**, 1174–1183.

Xie, B., Wang, X. and Hong, Z. (2010) Precocious pollen germination in *Arabidopsis* plants with altered callose deposition during microsporogenesis. *Planta*, **231**, 809–823.

Ye, Z.H. (2002) Vascular tissue differentiation and pattern formation in plants. *Annu. Rev. Plant Biol.* **53**, 183–202.

© 2010 The Authors